Available online at www.sciencedirect.com
SCIENCE DIRECT
Polymer 46 (2005) 6009–6015
polymer
www.elsevier.com/locate/polymer

Time resolved study of oriented crystallisation of poly(lactic acid) during rapid tensile deformation

A. Mahendrasingam[a,*], D.J. Blundell[a], M. Parton[a], A.K. Wright[a], J. Rasburn[b], T. Narayanan[c], W. Fuller[a]

[a]*School of Chemistry and Physics, Keele University, Staffordshire ST5 5BG, UK*
[b]*R&D Building, West Road, Innovia Films, Wigton, Cumbria CA7 9XX, UK*
[c]*ESRF, BP 220, F-38043 Grenoble Cedex, France*

Received 7 April 2005; accepted 18 May 2005
Available online 14 June 2005

Abstract

Poly(L-lactic acid) with 4% D-lactic acid comonomer has been drawn in the amorphous state at 80, 90, 100, 110 and 120 °C at an extension rate of 4 s^{-1} while simultaneously recording WAXS and SAXS patterns at intervals of 0.12 s. At 80, 90 and 100 °C, crystallisation is very rapid (1–4 s^{-1}) and follows a first order transformation process to give highly oriented crystals. SAXS patterns were barely detectable at these temperatures despite fractional crystallinity of ~0.2. At 110 and 120 °C, crystallisation was very slow (~0.01 s^{-1}) and gave rise to crystals with a lower degree of orientation. After eventual crystallisation at 120 °C, a two-point SAXS pattern develops with narrow lateral spread, suggesting 'shish kebab' morphology. When the 80 °C drawn sample was annealed at 120 °C, a strong four point SAXS pattern develops. The change in drawing and crystallisation behaviour at higher draw temperature is attributed to the onset of chain retraction relaxation processes. The WAXS fibre pattern after annealing shows sampling on intermediate layer lines that is consistent with the α crystal form with a 10_3 helix. However, prior to annealing, sampling indicates a different, less defined helical configuration.
© 2005 Elsevier Ltd. All rights reserved.

Keywords: Poly(lactic acid); WAXS; Crystallisation

1. Introduction

Poly(lactic acid) polymers are readily biodegradable, crystallisable thermoplastics with growing importance in biomedical and packaging applications [1]. The industrial processing of these materials often involves fabrication of oriented fibres or films [1].

From X-ray fibre diffraction α and β crystalline forms of poly(lactic acid) (PLA) have been identified. The structure of the α form was first determined by De Santis and Kovacs [2] to be pseudo orthorhombic with each unit cell containing two chains with a 10_3 helical conformation with $a=1.07$ nm, $b=0.645$ nm and $c=2.78$ nm. A later study of annealed fibres by Hoogsteen et al. [3] deduced slightly different parameters with $a=1.06$ nm, $b=0.61$ nm and $c=2.88$ nm. A similar unit cell was found by Marega et al. [4] from an analysis of a powder pattern. The β form was first identified by Eling et al. [5] and later shown by Hoogsteen et al. [3] to have an orthorhombic structure with each cell containing six chains with a 3_1 helical conformation and with $a=1.03$ nm, $b=1.82$ nm and $c=9.00$ nm. In an investigation of different drawing conditions, Hoogsteen et al. [3] found that the α form is favoured at low drawing temperatures and the β form at higher temperatures. More recently Korturk et al. [6] have studied tensile deformation of films between 60 and 80 °C at draw rates up to ~0.05 s^{-1} and found their samples crystallised in the β form. Several morphology studies of isotropic melt crystallised homopolymers and D-lactide and *meso*-lactid copolymers have shown lamellae crystals whose thickness decreases with increasing comonomer as a result of exclusion of comonomers from the lamellae [7–10]. Cicero et al. [11,12] studied melt spun fibres and found the morphology to be essentially microfibrillar. The earlier studies of Hoogsteen et al. [3] concluded that the fibrillar morphology

* Corresponding author. Tel.: +44 1782 583312; fax: +44 1782 712378.
E-mail address: a.mahendrasingam@keele.ac.uk (A. Mahendrasingam).

0032-3861/$ - see front matter © 2005 Elsevier Ltd. All rights reserved.
doi:10.1016/j.polymer.2005.05.081

was more associated with fibres with the β crystal form whereas fibres with the α form are more associated with the presence of oriented lamellae overgrowths.

This paper describes time-resolved WAXS and SAXS observations using a synchrotron X-ray source during the rapid tensile deformation of poly(L-lactic acid-*co*-4% D-lactic acid) (PLA) from the amorphous state. It is concerned with the kinetics of the development of crystallinity and the associated morphological changes and complements the previous studies. The time-resolved X-ray observations enable the development of crystallinity to be directly linked to the deformation process in real time. This approach has a major advantage over laboratory observations that are carried out after the completion of deformation and where structural development can occur post deformation (e.g. 6). Another important aspect of these experiments is the use of high deformation rates that are closer to the draw rates experienced in industrial processes. The same experimental technique has already been used successfully in our studies of deformation of amorphous poly(ethylene terephthalate) (PET) where the onset of the oriented crystallisation process was found to be dependent on the drawing conditions [13–16]. In particular the PET studies showed that when the deformation rate was faster than the chain retraction relaxation mechanism, the onset of crystallisation was delayed until the end of the deformation [14]. This contrasted with the use of slower draw rates where crystallisation commenced while deformation in still in progress.

The current experiments with PLA have been carried out over the temperature range 80–120 °C. They show that with increasing draw temperature there is a distinct change in the drawing behaviour and the resulting morphology when drawn above 100 °C.

2. Experimental

Experimental data were collected on beamline ID2A at the ESRF in Grenoble, France using X-ray wavelength λ of 0.0995 nm. The SAXS was collected on an image intensified CCD with a sample to detector distance of 3 m and was normalized to absolute intensities after applying different detector corrections. A second image intensified CCD was positioned at an oblique angle (32.5°) at a distance of about 120 mm to enable a sector of the WAXS pattern spanning an azimuthal angle of approximately 60° centred around the equator to be recorded simultaneously with the SAXS pattern.

The experiments were carried out in situ with the samples mounted in the jaws of a stretching device that had been purpose designed and constructed in the Keele Physics Department workshops [17,18]. The device is enclosed in an oven and the temperature is controlled to within 1 °C. The jaws of the stretching device were attached to stepper motors which allowed uniaxial, bi-directional drawing.

The polymer used for the study comprised poly (L-lactic acid) with ~4% D-lactic acid copolymerised units. The amorphous sheets of 0.8 mm thickness were formed by pressing commercial PLA pellets with ~4% D-content between Teflon-coated aluminium foils in a hot-press. After release from the hot-press, the sheet and foil assembly was quenched in a cold-water bath. Prior to melt processing, the pellets were dried overnight in a vacuum oven set at 100 °C. Specimens 10 mm wide were cut from the sheets and ink reference stripes were drawn with a separation of 1 mm on the specimen at right angles to the draw direction to enable the degree of extension to be deduced from a video camera image. The specimen was mounted in the jaws of the stretching device with a 10 mm gauge length.

The specimens were heated in the stretching device to the desired drawing temperature and allowed to equilibrate for 2 min before being drawn. They were then drawn to a nominal final draw ratio of around 4.5:1 at a draw rate of around 4 s^{-1}, during which 100 frames of 0.02 s duration were recorded sequentially every 0.12 s. The data for the 100 frames were then dumped before proceeding with the next experiment. The drawing experiments were carried out at five draw temperatures of 80, 90, 100, 110 and 120 °C. As indicated in Table 1, there were slight differences in the final draw ratio due to differences in the draw characteristics of the samples. In the case of the 120 °C experiment, the sample was maintained at 120 °C during the data dump and an additional static frame was recorded at 16 min after the end of the drawing process. In the case of the 80 °C experiment, the drawn sample was post-annealed in situ at 120 °C in order to further develop the morphology.

The kinetics of the crystallization process during the drawing were obtained from the variation in intensity of the strong equatorial reflection equivalent to the (200) reflection of the α crystalline form. The analysis was based on the curve fitting procedures developed previously in studies of PET [13–15]. The intensity data was scaled to give estimates of the absolute level of crystallinity by reference to an analysis of the whole WAXS pattern of the final frame of each experiment. The following procedure was used to obtain the crystallinity index of the reference sample. A randomised intensity $I(s)$ was obtained by summing the contributions of radial slices $i(s,\phi)$ taking account of axial symmetry:

$$I(s) = \sum_{\phi} i(s,\phi)\sin(\phi) \quad (1)$$

where ϕ is the azimuthal angle relative to the draw direction. As mentioned before the WAXS pattern covered only an azimuthal sector for $\phi < 60°$. Since the crystalline reflections were concentrated around the equator and the degree of amorphous orientation is very low, isotropic intensity distribution over the unrecorded angles was assumed to be identical to that recorded for 60°. The crystalline reflections and the amorphous diffraction were separated using the

Table 1
Drawing conditions and crystallisation data

Draw temperature (°C)	Final draw ratio	Crystallinity at end of draw	Crystallinity after further treatment at 120 °C	Crystallisation rate s^{-1}	Invariant after further treatment at 120 °C (mol electron)^2
80	4.1	.19	.21	1.1	2.0×10^{-4}
90	4.3	.25	–	4	–
100	5.2	.24	–	3.6	–
110	6.8	.02	–	.007	–
120	11	.02	.19	.004	2.4×10^{-4}

oriented pattern at the onset of crystallization as the amorphous reference. A crystallinity index for the total crystalline content was calculated from the ratio of the crystalline component relative to the total scattered intensity.

Estimates of the Invariant from the SAXS patterns were obtained by assuming the intensity function had uniaxial symmetry around the draw axis. The two dimensional pattern was projected on to the equatorial axis to obtain a one dimensional intensity profile $J(s)$, where s is the projected scattering vector defined by $s = 2\sin(\theta/\lambda)$. For the high-$s$ part of the scattering profile, it was assumed for simplicity that the decay of the $J(s)$ profile had a $1/s^3$ dependence. A constant background value B, due to random density fluctuations, was therefore chosen for subtraction from $J(s)$ so as to give the $1/s^3$ dependence. The invariant, $\langle\eta^2\rangle$, which is a measure of the fluctuation in electron density was then calculated from a summation based on

$$\langle\eta^2\rangle = 2\pi\int_0^\infty (J(s) - B)s\mathrm{d}s \tag{2}$$

where $J(s)$ was calibrated in absolute units.

3. Results

The observations revealed a distinct difference in the deformational response of the samples at 80, 90 and 100 °C compared with at 110 and 120 °C. At the lower draw temperatures, the deformation of the sample closely followed the applied deformation of the clamps. At the two higher temperatures, the central part of the sample at the position of the X-ray beam continued to deform non-uniformly after the end of the applied deformation. This resulted in an inhomogeneous draw. The variation of draw ratio at the position of the X-ray beam is indicated in Figs. 1–5 for each experiment.

The difference in deformational response was accompanied by a difference in the development of crystalline structure. An example of this difference is shown in Figs. 6 and 7, which show selected WAXS frames for drawing at 80 and 120 °C, respectively. In the 80 °C experiment shown in Fig. 6, the initial pattern in frame 1 shows a diffuse isotropic scatter typical of an amorphous polymer. During deformation there is an intensification of the diffuse scatter around the equator as in frame 6, indicating the alignment of polymer chains. Beyond the end of the deformation process at frame 7, there is a rapid growth of discrete crystalline reflections with low azimuthal spread typical of a well-oriented crystalline phase. By contrast in the 120 °C experiment shown in Fig. 7, there is no significant intensification of the diffuse amorphous scatter around the equator. The crystalline diffraction develops more slowly with a wider azimuthal spread indicating oriented crystals with poorer orientation. The last pattern shown in Fig. 7 is from the static observation recorded after a further 16 min at 120 °C and shows that significant further crystallisation has occurred. Interestingly, the additional crystals are less well oriented than in the initial crystal growth. There is also evidence of weak isotropic crystalline reflections in the initial frame at 120 °C indicating that a low level of crystallinity had developed during the temperature equilibration prior to deformation.

The development of crystallinity in all five experiments is shown in Figs. 1–5 alongside the local draw ratio at the X-ray beam position. At the three lower temperatures, the onset of crystallisation is close to the point where the deformation has ceased. The crystallinity then increases rapidly and then asymptotically reaching the final value. This behaviour is similar to that observed in our previous studies of PET homopolymer when drawn at these high deformation rates. Following the scheme developed in these previous studies [13,15], the crystallisation rate for the three lower temperatures was analysed in terms of the crystallisation kinetics of a first order transformation process fitted

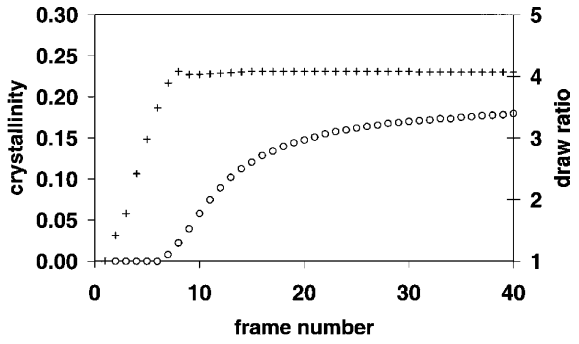

Fig. 1. Plots for experiment at 80 °C: ○, crystallinity; +, draw ratio. Each frame corresponds to a time interval of 0.12 s.

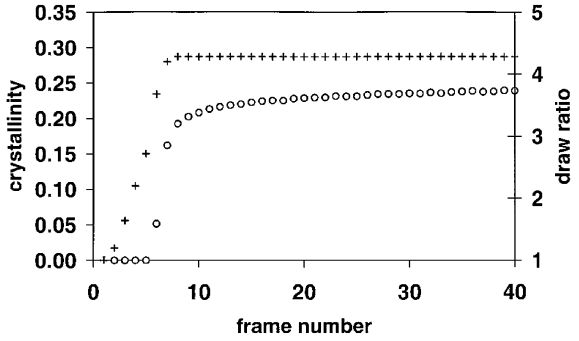

Fig. 2. Plots for experiment at 90 °C: ○, crystallinity; +, draw ratio. Each frame corresponds to a time interval of 0.12 s.

to the equation:

$$\frac{(\phi_\infty - \phi)}{\phi_\infty} = e^{-k(t-t_o)} \quad (3)$$

where ϕ_∞ represents the final attained crystallinity, ϕ is the crystallinity after time t, k is a rate parameter and t_o is the time of onset of crystallisation.

The data in Figs. 4 and 5 for 110 and 120 °C show a very slow rise in the crystallinity reaching only around 0.02 fractional crystallinity during the 12 s duration of the time-resolved observations. A closer scrutiny of the 120 °C experiment shows an initial faster crystallisation over 1.5 s followed by a much slower rise associated with less oriented crystals. The subsequent observation in the 120 °C experiment after a further 16 min show the fractional crystallinity eventually reaches around 0.2.

Estimates of the overall crystallisation rates are listed in Table 1. The values at the lower draw temperatures are derived from the parameter k in Eq. (3). The crystallisation rates for the two higher temperatures have been estimated from the linear increase in crystallinity in Figs. 4 and 5. These latter values are comparable with the crystallisation rates obtained by Kolstad [19] for isotropic polymer, suggesting that a similar growth mechanism is occurring in these cases.

The subsequent annealing at 120 °C of the sample initially drawn at 80 °C produces a small increase in

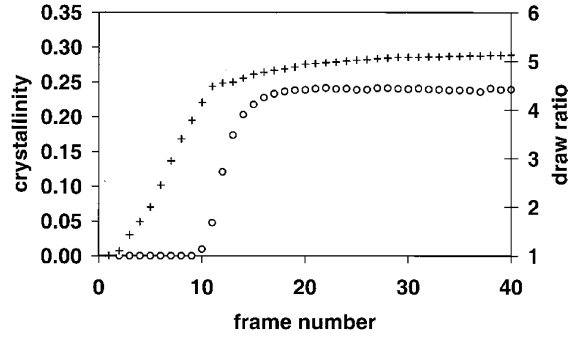

Fig. 3. Plots for experiment at 100 °C: ○, crystallinity; +, draw ratio. Each frame corresponds to a time interval of 0.12 s.

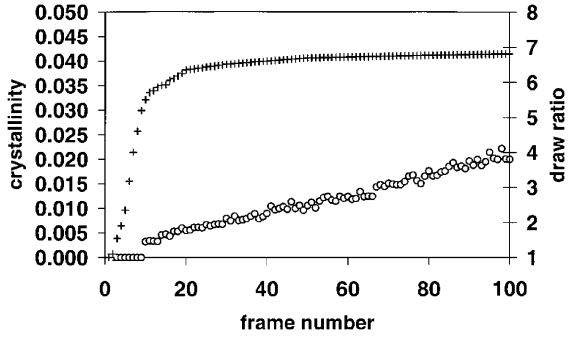

Fig. 4. Plots for experiment at 110 °C: ○, crystallinity; +, draw ratio. Each frame corresponds to a time interval of 0.12 s.

crystallinity with no reduction in the orientation of the crystals.

Fig. 8 shows a more detailed view of some of the WAXS fibre patterns and reveals the presence of fainter diffraction sampling between the main layer lines. Fig. 8(b) shows the well-developed pattern after annealing the 80 °C sample at 120 °C. The fainter diffraction is occurring on layer lines that are associated with a fibre repeat of around 3 nm. This is consistent with the α crystalline form with a 10_3 helix. Fig. 8(a) is from the final frame after drawing at 80 °C. In this case the additional diffraction is less well defined and appears to be displaced from the 3 nm layer lines, indicating a different helical configuration in the initial crystallised state. The presence of this extra diffraction also shows that the β crystalline form with the 3_1 helix is not occurring in this drawing experiment.

Surprisingly, SAXS patterns could not be readily resolved in any of the experiments during the time resolved observations. However, after the further 16 min in the 120 °C experiment a clear two-point SAXS pattern developed as in Fig. 9(a). The two diffraction maxima have a narrow lateral width and correspond to a meridional spacing of 20.9 nm. A clear pattern also developed when the 80 °C drawn sample was annealed at 120 °C as in Fig. 9(b). This consists of a four-point pattern with a resolved meridional spacing of 17.5 nm. A close scrutiny of the final SAXS frame after drawing at 80 °C does reveal a very

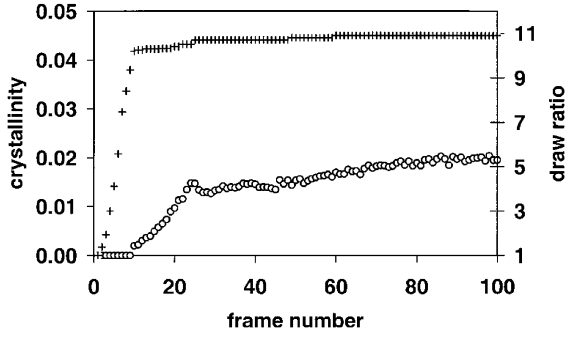

Fig. 5. Plots for experiment at 120 °C: ○, crystallinity; +, draw ratio. Each frame corresponds to a time interval of 0.12 s.

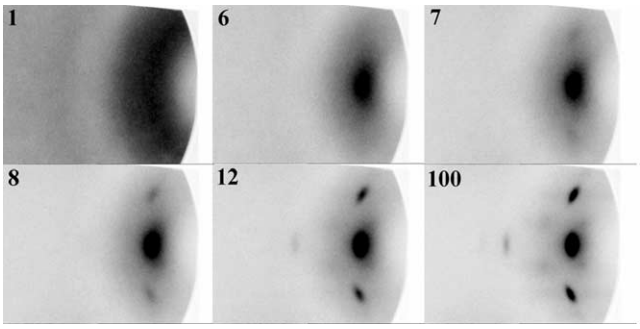

Fig. 6. WAXS pattern from 80 °C experiment showing frames 1, 6, 7, 8, 12 and 100.

faint, less developed pattern with a four-point character but the intensity statistics is not adequate for detailed analysis.

4. Discussion

The low crystal orientation and the low crystallisation rate at the higher draw temperatures can be attributed to greater chain mobility resulting in increased relaxation. At the lower draw temperatures, the oriented crystallisation process is characterised by kinetics, which is reminiscent of a first order transformation process in which the onset of crystallisation is delayed until near the completion of the main deformation. This characteristic is similar to that found in our previous studies of fast tensile deformation of amorphous PET when drawn around 15–30 °C above its T_g [13–15]. An analysis of known chain relaxation processes in PET led us to conclude that the deformation is occurring in a regime where the extensional strain rate is comparable to, or, faster than the chain retraction mechanism [14]. It is therefore not unreasonable to propose that the deformation of PLA below 100 °C at rates $\sim 4\ s^{-1}$ is also occurring in an analogous regime of chain relaxation. Accordingly the change in behaviour above 100 °C could therefore be associated with a significant degree of chain retraction during the drawing process in which only the very highest molecular weight chains are able to achieve significant extension.

In this respect it is of interest to compare our current

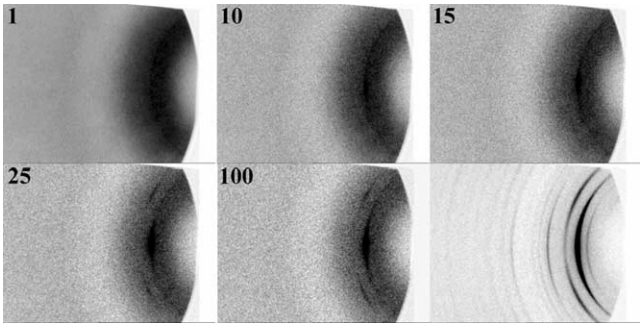

Fig. 7. WAXS pattern from 120 °C experiment showing frames 1, 10, 15, 25 and 100 and the static frame taken 16 min after the end of the deformation.

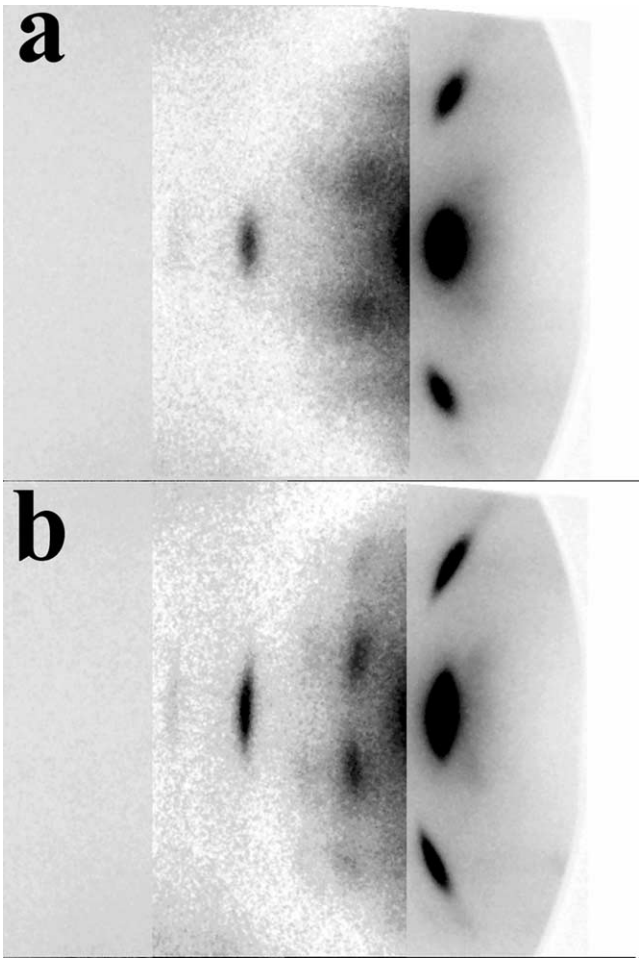

Fig. 8. WAXS patterns where the central section is intensified to show diffraction on intermediate lines: (a) final frame after drawing at 80 °C; (b) Sample drawn at 80 °C and then annealed at 120 °C.

observations with the results of Korturk et al. [6] in their study of tensile deformation at the much slower strain rate of $\sim 0.05\ s^{-1}$. Their WAXS diffraction patterns for drawing at 70 °C to draw ratios around 4:1 are very similar to those in Fig. 6. At 70 °C, the time–temperature shift factor will significantly change the relaxation times of the chain retraction mechanisms. The dielectric relaxation experiments of Kanchanasopa and Runt [20] indicate that raising the temperature from 70 to 80 °C will reduce the relaxation time of the α-relaxation by a factor of around 100. It is therefore likely that the oriented crystallisation process occurring in the studies of Kokturk et al. [6] will be in a similar relaxation regime to that occurring in Fig. 6.

The very low intensity of the SAXS during the time resolved drawing is at first sight surprising, particularly in the case of the low temperature drawing experiments where significant levels of crystallinity are achieved during the observation period. It is less surprising for the higher temperature drawing where only a very low level of crystallinity is achieved within the 12 s duration of the experiment. According to crystallographic studies in the

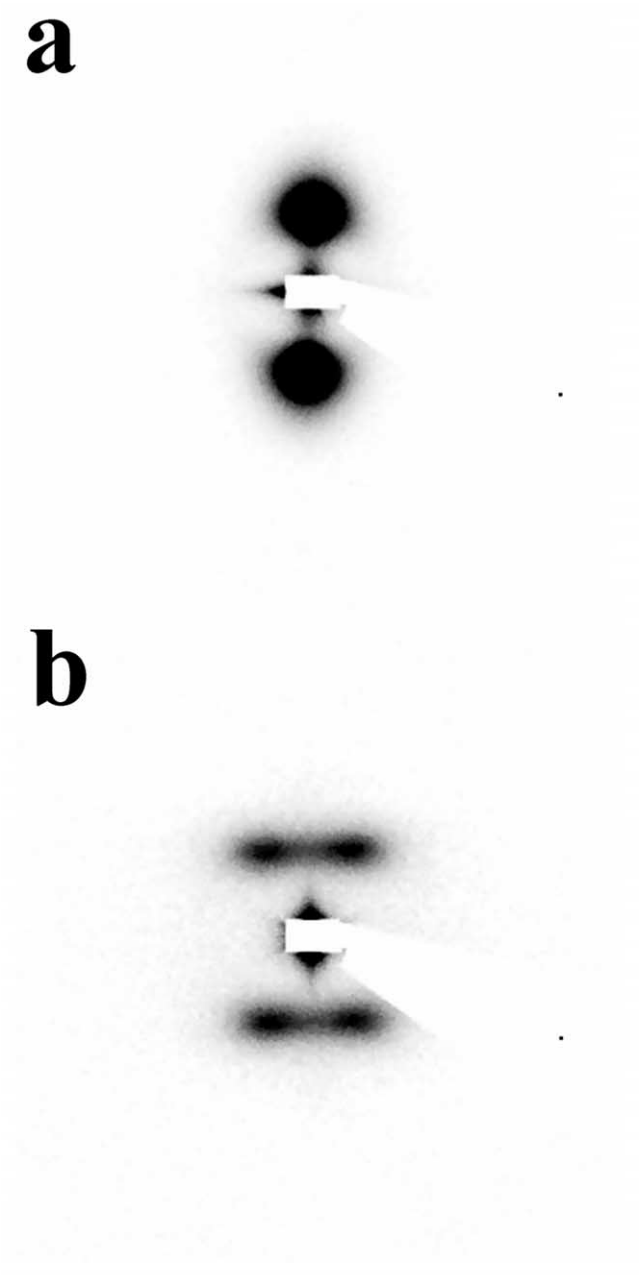

Fig. 9. SAXS patterns showing (a) two-point pattern in 120 °C experiment at 16 min after drawing and (b) four-point pattern for sample from 80 °C experiment during subsequent annealing at 120 °C.

literature, the densities ρ_c of the α crystalline cell is 1.283 g/ml [3]. According to Fischer et al. [21] the density of amorphous polymer ρ_a is 1.248 g/ml. The difference in density $\Delta\rho \sim 0.035$ g/ml is very small compared to most polymers and therefore the scattering contrast is very low to observe SAXS above the background level within a short integration time of 0.02 s. The density difference and the contrast would become even smaller if the crystalline density is reduced due to imperfections or if the non-crystalline parts are increased due to strain, both of which could be occurring during the low temperature draw. The appearance of clear SAXS patterns after annealing at 120 °C could therefore be due to improved crystal perfection and increased ρ_c, or, more relaxed non-crystalline regions and lower ρ_a. In the cases of the annealed 80 °C sample and the 16 min observation of the 120 °C sample, the estimated invariant is given by $\langle\eta^2\rangle \sim 2\times10^{-4}$ (mol electron/cm^3)^2. According to a two phase model, the invariant is given by:

$$\langle\eta^2\rangle = \phi(1-\phi)\Delta\rho_e^2 \quad (4)$$

where $\Delta\rho_e$ is the electron density difference and ϕ is the phase volume. Assuming the crystalline phase occupies a volume fraction of $\sim$0.2, this infers a mass density difference of $\sim$0.07 g/ml. This is significantly larger than the above quoted density difference between the crystalline and amorphous phases. However, the discrepancy can be accounted for by the differential thermal expansions of the two phases. There are no data available for PLA but significance of this effect can be inferred from polyethylene data of Grubler [22] where the differential volume expansion coefficient between the crystals and liquid melt was found to be $\sim 6\times10^{-4}$/°C. The observation temperature of 120 °C is about 60 °C above the T_g of PLA. This temperature interval would therefore be expected to enhance the density difference by about 0.036 g/ml and would thus explain the discrepancy.

The comparison between the SAXS patterns in Fig. 9 indicates a significant difference in morphology between the higher and lower draw temperatures. The four point patterns after annealing of the low temperature draw is similar to that seen in very highly drawn PET where there is a microfibrillar morphology. On the other hand, two point patterns with a narrow lateral width have often been attributed to an oriented lamellar morphology. For example, such a morphology has been seen to occur in polyethylene that has been gel-spun or stirrer-crystallised from solution and has been shown to be associated with stacks of lamellar 'kebab' overgrowths that have been nucleated on 'shish' cores. This difference suggest that the low temperature drawn samples have a microfibrillar morphology, similar to those seen by Cicero et al. [11,12], whereas the samples drawn at high temperatures are closer to a shish–kebab morphology.

5. Conclusions

Samples drawn at the lower temperatures of 80, 90 and 100 °C show different drawing and crystallisation behaviours to the higher temperature draws at 110 and 120 °C. The change in behaviour above 100 °C is attributed to the onset of relaxations associated with chain retraction mechanisms.

At the lower temperatures, there is a rapid crystallisation giving highly oriented crystals with the crystallisation

kinetics following a first order transformation process. Clear SAXS patterns could not be detected during the 12 s duration of the time-resolved observations. This was partly due to the poor density contrast between crystalline and non-crystalline regions. Annealing treatment improves the contrast and gives rise to a clear four-point SAXS pattern, suggesting a microfibrillar morphology in the as-drawn sample.

At the higher temperatures, the draw is non-uniform and gives rise to less oriented crystals with a very slow growth rate. Prolonged crystallisation after drawing at 120 °C gives a two-point SAXS pattern indicating a 'shish–kebab' morphology.

The WAXS fibre pattern after annealing shows a sampling on intermediate layer lines that is consistent with the α crystal form with a 10_3 helix. However, prior to annealing the sampling indicates a different helical configuration.

Acknowledgements

This work was supported by the allocation of beam time at the ESRF. We are grateful to M.G. Davies, E.J.T. Greasley, and M.P. Wallace for technical support.

References

[1] Garlotta D. J Polym Environ 2002;9:63.
[2] De Santis P, Kovacs AJ. Biopolymers 1968;6:299.
[3] Hoogsteen W, Postmen AR, Pennings AJ, Brinke G, Zugenmaier P. Macromolecules 1990;23:634.
[4] Marega C, Marigo A, DiNoto V, Zannetti R. Makromol Chem 1992; 193:1599.
[5] Eling B, Gogolewski S, Pennings AJ. Polymer 1982;23:1587.
[6] Korturk G, Serhatkulu TF, Cakmak M, Piskin E. Polym Eng Sci 2002; 42:1619.
[7] Huang J, Lisowski MS, Runt J, Hall ES, Kean RT, Buehler N, et al. Macromolecules 1998;31:2593.
[8] Barantian S, Hall ES, Lin JS, Xu R, Runt J. Macromolecules 2001;34: 4857.
[9] Kanchanasopa M, Manias E, Runt J. Biomacromolecules 2003;4: 1203.
[10] Cho JD, Barantian S, Kim J, Yeh FJ, Hsiao BS, Runt J. Polymer 2003; 44:711.
[11] Cicero JA, Dorgan JR, Janzen J, Garrett J, Runt J, Lin JS. J Appl Polym Sci 2002;86:2828.
[12] Cicero JA, Dorgan JR, Garrett J, Runt J, Lin JS. J Appl Polym Sci 2002;86:2839.
[13] Blundell DJ, Mackerron DH, Fuller W, Mahendrasingam A, Martin C, Oldman RJ, et al. Polymer 1996;37:3303.
[14] Blundell DJ, Mahendrasingam A, Martin C, Fuller W, MacKerron DH, Harvie JL, et al. Polymer 2000;41:7793.
[15] Mahendrasingam A, Blundell DJ, Martin C, Fuller W, MacKerron DH, Harvie JL, et al. Polymer 2000;41:7803.
[16] Mahendrasingam A, Blundell DJ, Wright AK, Urban V, Narayanan T, Fuller W. Polymer 2003;44:5915.
[17] Mahendrasingam A, Fuller W, Forsyth VT, Oldman RJ, Mackerron DH, Blundell DJ. Rev Sci Instrum 1992;63:1087.
[18] Hughes DJ, Mahendrasingam A, Martin C, Oatway WB, Heeley EL, Bingham SJ, et al. Rev Sci Instrum 1999;70:4051.
[19] Kolstad JJ. J Appl Polym Sci 1996;62:1079.
[20] Kanchanasopa M, Runt J. Macromolecules 2004;37:863.
[21] Fischer EW, Sterzel HJ, Wegner G. Kolloid ZuZ Polym 1973;251: 980.
[22] Grubler M. Thesis-La structure du polyethylene ses variations avec les caracteristiques moleculaires et l'histoire thermique des echantillons. University of Strasbourg; 1961.